RSC Pharmaceutics

ROYAL SOCIETY OF CHEMISTRY

PAPER

View Article Online
View Journal | View Issue

Check for updates

Cite this: *RSC Pharm.*, 2025, **2**, 318

Design and evaluation of solid self-nanoemulsifying drug delivery systems of cyclosporine developed with a superior adsorbent base†

Mohit Kumar, [a] Pooja A. Chawla, *[b] Abdul Faruk[a] and Viney Chawla[b]

Cyclosporine (CYC) is a drug that belongs to the BCS class II category. This study was designed to develop novel solid self-nanoemulsifying drug delivery systems (S-SNEDDS) for cyclosporine (CYC), using chitosan–EDTA microparticles. Such microparticles are known to exhibit superior adsorbent characteristics and were prepared by two different methods *viz*. spray drying (SD-CHEM) and solvent evaporation (SE-CHEM). Capmul® GMS-50K, Labrafac, and PEG 400 were chosen as the oil, surfactant, and co-surfactant, respectively. The cyclosporine liquid self-nanoemulsifying drug delivery system (CYC-L-SNEDDS) was developed with an optimal oil to S_{mix} (surfactant : co-surfactant) ratio of 40 : 60, determined through a pseudo ternary phase diagram. The novel S-SNEDDS were developed by adsorbing CYC-L-SNEDDS onto the chitosan–EDTA microparticles, resulting in CYC-SD-S-SNEDDS and CYC-SE-S-SNEDDS. Both formulations exhibited favorable drug loading, with 81.184 ± 4.191% for CYC-SD-S-SNEDDS and 56.426 ± 5.471% for CYC-SE-S-SNEDDS. XRD and DSC confirmed drug amorphization, while SEM revealed a smooth, well-distributed adsorbate on the adsorbent surfaces, with particle sizes of 5–8 μm for CYC-SD-S-SNEDDS and 10–12 μm for CYC-SE-S-SNEDDS. When tested for stability, the developed formulations exhibited excellent physical and thermodynamic stability. The globule size for CYC-SD-S-SNEDDS was 138.7 ± 4.14 nm, with a PDI of 0.613 ± 0.004, while CYC-SE-S-SNEDDS had a globule size of 166.9 ± 4.04 nm and a PDI of 0.579 ± 0.003. The results of *in vitro* dissolution studies revealed that there was a fourfold increase in drug dissolution for CYC-SD-S-SNEDDS (80.03%) and CYC-SE-S-SNEDDS (72.26%) when compared to the pure cyclosporine (19.8%). A similar pattern was observed in *ex vivo* permeation studies where CYC-SD-S-SNEDDS showed 39.34% release and CYC-SE-S-SNEDDS exhibited 28.31% release as compared to CYC-L-SNEDDS (41.46%). Furthermore, CYC-SD-S-SNEDDS outperformed CYC-SE-S-SNEDDS, indicating the superiority of microparticles developed by the spray drying method (SD-CHEM) as adsorbents for solidification. These findings suggest enhanced dissolution and permeation for cyclosporine in S-SNEDDS.

Received 9th July 2024,
Accepted 26th November 2024

DOI: 10.1039/d4pm00198b

rsc.li/RSCPharma

1. Introduction

Cyclosporine (CYC) was first isolated by Sandoz from the crude extracts of *Tolypocladium inflatum gams* fungus.[1] It is an oligopeptide with 11 amino acids and has a molecular weight of 1202 Da. CYC has immunomodulatory properties and prevents allograft rejection after organ transplants and increases the survival of such patients in the initial and long run. It is also used in autoimmune and inflammatory disorders.[2] CYC is a calcineurin inhibitor and selectively suppresses different T-lymphocytes' functions especially the generation of interleukin-2.[3] CYC forms a cyclosporine–cyclophilin complex after binding to cyclophilin and by inhibiting calcineurin phosphatase and T-cell activation, it suppresses immunity.[4]

CYC is a BCS (biopharmaceutical classification system) class II drug with low hydrophilicity (slightly soluble in water, 0.04 mg g^{-1})[5] and high lipophilicity.[6] The extent of bioavailability is significantly influenced by the solubility of the drug in the gastrointestinal tract[7] (GIT). When taken orally, it has high variability in bioavailability from 20 to 60%.[8] The high difference in interpersonal variation in pharmacokinetic parameters is because CYC distribution gets affected by factors like population, age, nutrients, gender, and administration

[a]*Department of Pharmaceutical Sciences, HNB Garhwal University, Srinagar, Garhwal, 249161 Uttarakhand, India*
[b]*University Institute of Pharmaceutical Sciences and Research, Baba Farid University of Health Sciences, Faridkot, 151203 Punjab, India. E-mail: pvchawla@gmail.com*
† Electronic supplementary information (ESI) available. See DOI: https://doi.org/10.1039/d4pm00198b

with other medications.[9] Sandimmune® and Neoral® are the two products commercially available for the oral delivery of this medication. They have been incorporated into a self-nanoemulsifying drug delivery system (SNEDDS) known as a "microemulsion", utilizing either soft or hard capsules. The primary distinction between these two formulations lies in the distribution of particle sizes. The globule sizes in Sandimmune® vary from a few nanometres to several micrometres, whereas Neoral® exhibits a more uniform sized system with globule sizes ranging from 100 to 250 nm.[10]

SNEDDS exhibit a substantial capability to enhance the oral bioavailability and biological effectiveness of drugs that exhibit poor water solubility.[11,12] In addressing the challenge of enzymatic degradation in the gastrointestinal tract during the oral delivery of biomolecules (proteins and peptides), lipid-based systems like SNEDDS have demonstrated efficacy.[13] SNEDDS present numerous challenges and difficulties, including physical and chemical instability issues. The liquid form of SNEDDS (L-SNEDDS) presents several challenges, including limitations on manufacturing dosage, limited options for dosage forms, low drug loading capacity, and complex challenges in handling and storage.[14,15] The most common technique for encapsulating liquid or semi-solid lipid-based formulations intended for oral administration is filling in capsules. This method is suitable for highly potent drugs and enables a moderately high drug loading, constrained by both the fill weight and the drug's solubility.[16] Nevertheless, capsule technologies come with specific drawbacks, mainly when co-solvents are involved; it is essential to consider the interaction between the shell and the filling. Such factors contribute to a slower manufacturing process and higher costs than other solid dosage forms such as tablets.[17]

Due to these limitations, researchers and formulators consistently explore diverse methods to solidify the L-SNEDDS, facilitating a solid product's rapid and straightforward development with the desired properties.[18] Solid self-nanoemulsifying drug delivery systems (S-SNEDDS) are established and recognized formulation systems. Common adsorbents are polyvinyl alcohol, sodium CMC, dextrin, β-cyclodextrin, lactose, mannitol, HP-β-CD, maltodextrin, PVP K-30, Aerosil-200, Avicel PH102, Syloid XDP 3150, Neusilin US2, Syloid 244FP and magnesium stearate.[19] Some of the common SNEDDS (hard and soft capsules) available in the market are Gengraf® (cyclosporine, AbbVie Inc.), Lipirex® (atorvastatin, Highnoon Laboratories Ltd), Convulex® (sodium valproate, Gerot Lannach UK Limited), Norvir® (ritonavir, AbbVie Inc.), Rocaltrol® (calcitriol, Aphena Pharma Solutions), Sandimmune® (cyclosporine, Novartis Pharmaceuticals Corporation), Neoral® (cyclosporine, Novartis Pharmaceuticals Corporation), Vesanoid® (tretinoin, Roche Laboratories Inc.), Accutane® (isotretinoin, Roche Laboratories Inc.), and Agenerase® (amprenavir, GlaxoSmithKline).

S-SNEDDS provide numerous benefits, including an enhanced surface area (resulting in high solubility and bioavailability), robustness, high stability, scalability, ease of handling, high drug loading, improved flowability, reduced drug precipitation, and cost-effective production[20,21] as compared to L-SNEDDS. Therefore, the present research focused on developing an S-SNEDDS of the CYC (with the adsorption technique using superior microparticles developed by spray drying and solvent evaporation) having high solid form characteristics and similar dissolution and permeation profiles of reconstituted nanoemulsions from the S-SNEDDS as compared to L-SNEDDS. This approach will offer a stable S-SNEDDS of CYC that delivers comparable dissolution and permeation profiles to those of L-SNEDDS, but without the limitations associated with the liquid form.

2. Materials and methods

Cyclosporine was a gift sample from Panacea Biotec (New Delhi, India) with >95.6% purity. Capmul® GMS-50K (glyceryl monostearate), Caprol® ET (hexaglycerol octasterate), Captex® 200 (propylene glycol dicaprylate), and Captex® 300 (glyceryl tricaprylate/tricaprate) were gift samples from Abitech (USA). Labrafac™ PG (propylene glycol dicaprylocaprate) from Gattefossé (Canada) was also received as a gift sample. Polyethylene glycol 400 (PEG 400) was procured from TCI (India). Propylene glycol and ethylene diamine tetra acetic acid disodium (EDTA disodium) were obtained from CDH (New Delhi, India). Chitosan with 90% deacetylation (DA) was acquired from Marine Hydrocolloids (Kerala, India). Cremophor® RH-40 (polyoxyl 40 hydrogenated castor oil) was procured from HiMedia (Mumbai, India). Lipoxol 300 (PEG 300) was obtained from Sasol Chemicals (Texas, USA). Apart from those specifically mentioned, analytical-grade chemicals were used for the study. They were used as received.

2.1. Drug solubility investigation in different excipients

Cyclosporine is a high-dose medicament, so it is essential to achieve maximum drug-loading capacity in the L-SNEDDS formulation. To obtain and plot the emulsification region, it was important to investigate the saturation solubility of cyclosporine in different excipients. An excess amount of the drug was taken in a screw-capped vial. The vials were treated in a water bath at 40 °C for 15 minutes. The mixture was blended in an orbital shaker incubator (Remi, India) at 100 rpm for 72 hours at room temperature.[22] After this, the mixture was centrifuged (Remi RC-8, India) at 4000–5000 rpm for 30 minutes at room temperature. The supernatant obtained was passed through Whatman filter paper (0.45 μm nylon). After appropriate dilutions, the amount of cyclosporine was quantified at 209 nm using a UV spectrophotometer (UV-VIS spectrophotometer-2371 EI, India). The experimental study was performed in triplicate.[23]

Self-emulsification potential is also a crucial criterion for selecting excipients in L-SNEDDS, along with the high solubility of the drug in oil and surfactant. For that, a 10% w/v solution of each surfactant (that showed high drug solubility) was prepared. This solution (10 ml) was taken and titrated with each oil. The oil volume was noted where it turned the emulsion turbid. The oil

and surfactant combination, which emulsified a high amount (of oil), was selected.[24] The S_{mix} (1 : 1) ratio of the selected surfactant was formed with each co-surfactant (which showed high solubility with the drug). With this S_{mix}, several formulations were made from the selected oil ranging from 10 to 90% in concentration. 500 mg of each formulation was taken and mixed separately in 500 ml of triple distilled water, and transparency or appearance of the mixture was observed.[25]

2.2. Pseudo-ternary phase diagram

A pseudo-ternary phase diagram was plotted to determine the range of excipients for nanoemulsion formation. The total entirety of ternary mixtures prepared with three ingredients (including an equal amount of drug) was kept at 1 g. The selected surfactant and co-surfactant were mixed in 1 : 1, 1 : 2 and 2 : 1 ratios as S_{mix} mixtures. The oil and each S_{mix} proportions were blended in a total of nine different weight proportions varying from 1 : 9 to 9 : 1 in separate glass vials. The objective was to establish the most extreme proportions for the examination, aiming to delineate the boundaries of phase accuracy within this diagram. Each formulation was titrated with 500 ml of triple distilled water to observe the nanoemulsion formation. The transparent/clear solution confirmed nanoemulsion formation. The proportions of oil and S_{mix} were noted and are presented in the diagram. Chemix software was used to plot the diagram, and ingredients addressed sides of this diagram.[26]

2.3. Preparation of the self-nanoemulsifying drug delivery system

The correct proportion of the oil and S_{mix} was selected from the pseudo-ternary phase diagram experiment to produce a self-nanoemulsifying drug delivery system. The constituents selected were Capmul® GMS-50K (as the oil), Labrafac (as the surfactant) and PEG 400 (as the co-surfactant). Furthermore, a liquid self-emulsifying nano-drug delivery system of cyclosporine (CYC-L-SNEDDS) was prepared. The weighed amount of the drug was gradually added to the oil in a beaker and stirred at 2000 rpm on a magnetic stirrer until a homogeneous solution was formed. To this solution, 1 : 1 S_{mix} was added dropwise under constant stirring for 30 minutes to form an isotropic mixture. It was equilibrated for 48 hours at ambient temperature and was observed for the phase separation.[27]

2.4. Formation of the solid self-nanoemulsifying drug delivery system

In our previous research work, we optimized and developed superior adsorbent chitosan–EDTA microparticles by spray drying (SD-CHEM) and chitosan–EDTA microparticles by the solvent evaporation method (SE-CHEM).[28] These microparticles showed high oil adsorption capacity and oil desorption capacity and their surface free energy components analysis showed enhanced dispersive components and dynamic advancing contact angles, which are favorable properties for the adsorbent base to solidify the L-SNEDDS to S-SNEDDS.

Briefly, for SE-CHEM, chitosan–EDTA disodium solution (60 : 40) was subjected to solvent evaporation in a rotary evaporator (Micro Technologies, India) at a drying temperature of 70 °C for 45–60 minutes; then, the dry film was scrapped carefully and dried in an oven to remove the residual moisture for 40–50 minutes at 70 °C. The dried film was converted into powder by using a pestle mortar. For SD-CHEM, chitosan–EDTA disodium solution (50 : 50) was subjected to an inlet temperature of 110 °C, aspirator speed of 1000–2000 rpm, atomisation pressure of 3 kg cm^{-2} and feed pump at 15 rpm in a spray dryer (SprayMate JISL, India). In the continuity of our research work, the developed L-SNEDDS of CYC was fabricated, with the adsorption or solid carrier technique, to create an S-SNEDDS. These microparticles SD-CHEM and SE-CHEM were used as adsorbents, and CYC-L-SNEDDS as the adsorbate. The CYC-L-SNEDDS was added sequentially to SD-CHEM and SE-CHEM separately and rigorously mixed in a mortar and pestle to form CYC-SD-S-SNEDDS (cyclosporine solid self-nanoemulsifying drug delivery system with spray dried microparticles) and CYC-SE-S-SNEDDS (cyclosporine solid self-nanoemulsifying drug delivery system with solvent evaporated microparticles).[29] The ratio of the adsorbate (CYC-L-SNEDDS) : adsorbent (SD-CHEM and SE-CHEM) was optimised to get non-sticky, free-flowing powders *viz.* CYC-SD-S-SNEDDS and CYC-SE-S-SNEDDS, respectively.

2.5. Evaluation of the CYC-L-SNEDDS, CYC-SD-S-SNEDDS and CYC-SE-S-SNEDDS

2.5.1. Drug loading efficiency (%). To evaluate the drug loading efficiency (%), 100 mg of the CYC-L-SNEDDS, CYC-SD-S-SNEDDS and CYC-SE-S-SNEDDS were taken differently in 10 ml of methanol and vortexed in an orbital shaker (Remi, India) for 10 minutes. The CYC-L-SNEDDS mixture in methanol was directly analysed after suitable dilution and analyzed at 209 nm using a UV spectrophotometer (UV-VIS spectrophotometer-2371 EI, India). The remaining two mixtures were centrifuged (Remi Rc-8, India) at 4000 rpm for 10 minutes, and the supernatant obtained was passed through Whatman filter paper (0.45 μm nylon). After the dilutions of the withdrawn samples (in the range below 100 μg ml^{-1}), these were analysed in a UV spectrophotometer and performed in triplicate.[29] The drug loading efficiency (%) was calculated by using the equation:

$$\text{Drug loading efficiency}\,(\%) = \frac{\text{Actual quantity of drug present in the known amount of formulation}}{\text{Initial drug load}} \times 100a \quad (1)$$

2.5.2. Flow properties. For both the CYC-SD-S-SNEDDS and CYC-SE-S-SNEDDS, the angle of repose (fixed funnel method), apparent bulk density, tapped density, Carr's index and Hausner's ratio were calculated by standard methods to report flow properties.[30]

2.5.3. Solid state characterisation

2.5.3.1. X-ray diffraction analysis. X-ray diffraction (XRD) graphs of the pure CYC, SD-CHEM, SE-CHEM, CYC-SD-S-

SNEDDS and CYC-SE-S-SNEDDS were obtained using an X-ray diffractometer (XRD Aeris, Malvern Panalytical, UK). The samples were filled in a sample holder well and pressed properly; an extra amount of sample was removed using a glass slide and the bottom of the sample holder (lid) was fixed. These were scanned continuously from 10° to 50° at a rate of 2° per minute, with 0.02°2θ increments in an X-ray diffractometer. The scanning was initiated at 10° and concluded at 50° (2θ). The scans were conducted at 25 °C, configuring the generator at 45 kV.[29]

2.5.3.2. Surface morphology. The surface morphology and topography of the CYC, SD-CHEM, SE-CHEM, CYC-SD-S-SNEDDS and CYC-SE-S-SNEDDS were observed using a scanning electron microscope (SEM) (ZEISS Sigma 360, Germany) at 20 kV (EHT).[31] The samples were fixed on the SEM stub and coated with a thin layer of gold. Various images were obtained at different magnifications.

2.5.4. FTIR analysis. Various formulation components, along with their physical mixtures, were assessed for potential incompatibilities using a KBr pellet measured at ambient temperature in the 500–4000 cm^{-1} spectral range in FTIR-ATR analysis (FTIR PerkinElmer spectrum two, USA).[32]

2.5.5. DSC analysis. The DSC thermograms for CYC, CYC-SD-S-SNEDDS and CYC-SE-S-SNEDDS were recorded in a differential scanning calorimeter (DSC-25 TA, USA) in the 40–400 °C temperature range with 10 °C per minute heating rate under a nitrogen atmosphere.

2.5.6. Evaluation of the reconstituted nanoemulsion and CYC-L-SNEDDS. To determine the reconstitution ability, 100 mg of CYC-SD-S-SNEDDS and CYC-SE-S-SNEDDS were dispersed differently in 100 ml of triple distilled water for 1 h and later vortexed in an orbital shaker (Remi, India) for 10 minutes. This developed suspension was centrifuged (Remi RC-8, India) at 4000 rpm for 10 minutes to remove the undissolved particles, and the supernatant obtained was reconstituted as a nanoemulsion and used for further investigations. The 1 : 100 w/v dilution of the freshly prepared CYC-L-SNEDDS was made with triple distilled water and dispersed and used for further analysis.

2.5.6.1. Determination of globule size, size distribution and zeta potential. The globule size, polydispersity index and zeta potential of the reconstituted nanoemulsions and CYC-L-SNEDDS were analysed for zeta potential on a Zetasizer Nano ZS at 633 nm at 25 °C (Malvern Panalytical, UK). This procedure was carried out in triplicate and presented as the mean ± standard deviation.[33,34]

2.5.6.2. Self-emulsification time. The supernatants of the reconstituted nanoemulsion from CYC-SD-S-SNEDDS, CYC-SE-S-SNEDDS and liquid CYC-L-SNEDDS (1 ml sample) was each dispersed into 500 ml of triple distilled water and stirred at around 100 rpm with a magnetic stirrer. The observation was made regarding the formation of emulsion and the time required for dispersibility.[35]

2.5.6.3. Percent transmittance test. When L-SNEDDS are prepared for the oral route, there are chances that the drug after dilution in the gut lumen may get precipitated, for which the percent transmittance test is carried out. The supernatants of the CYC-L-SNEDDS, CYC-SD-S-SNEDDS and CYC-SE-S-SNEDDS were determined for percent transmittance at 209 nm against water as a blank using a UV spectrophotometer (UV-VIS spectrophotometer-2371 EI, India) and performed in triplicate.[36,37]

2.5.6.4. Cloud point estimation. The supernatant from CYC-L-SNEDDS, CYC-SD-S-SNEDDS, and CYC-SE-S-SNEDDS was placed in a water bath with a gradual temperature increase. The temperature point was noted where instant turbidity appeared in the samples.[38]

2.5.6.5. Field emission scanning electron microscopy. 50 µl of supernatant from each CYC-SD-S-SNEDDS and CYC-SE-S-SNEDDS were dropcast onto previously washed and cleaned glass slides. The dried samples were coated with gold using a sputter-coater for 10–15 seconds in a high vacuum. The images (high-resolution) were captured at 15 kV with an accelerating voltage by field emission scanning electron microscopy (FE-SEM) (Quanta 250, Bruker).[39]

2.5.6.6. In vitro dissolution study. In hard gelatin capsules (capsule size 00), the pure CYC, CYC-L-SNEDDS, CYC-SD-SNEDDS and CYC-SE-SNEDDS, equivalent to 10 mg, were filled separately to determine the CYC release by using the USP dissolution apparatus II-paddle at 37 ± 0.5 °C (Electrolab India, India) in triple distilled water as the dissolution medium with 50 rpm stirring speed (as per the method mentioned in USP). At different time intervals, 2 ml of sample aliquot was withdrawn (instantly filtered), and fresh medium was introduced to maintain sink conditions. After proper dilution with methanol, samples were analysed at 209 nm using a UV spectrophotometer.[40] In order to achieve a consistent and precise average value, the experiments were conducted three times.

2.5.6.7. Ex vivo permeation study. The *ex vivo* permeation method reported by Singh *et al.* (2013) was followed.[41] Briefly, the biological membrane of porcine small intestine (obtained from the local slaughterhouse, Srinagar Garhwal Uttarakhand, India) was used as a diffusion barrier and utilised within 1 hour of the slaughter. Kreb's ringer phosphate solution was used for intestine storage at 4 °C by providing aeration from aerators. Around 10–12 cm portion of the porcine small intestine was removed by cutting with scissors and (after washing with saline) placed on saline-soaked filter paper. A lengthwise cut was made to separate the intestine to flatten it. The serosal membrane was kept upward, and by using a scalpel, the muscle layer was removed. A modified Franz diffusion cell was used after mounting the intestine member (the mucosal layer facing the donor compartment side) for the permeation study. The triple distilled water in the receptor compartment was used as a receptor medium kept at 37 ± 0.5 °C and stirred at 50 rpm. The donor compartment was added with pure CYC/CYC-L-SNEDDS/CYC-SD-S-SNEDDS/CYC-SE-S-SNEDDS (5 mg equivalent of CYC) to the mucosal side of the membrane with little stir. At different time intervals, a 1 ml sample was withdrawn and replaced with fresh 1 ml triple distilled water in the receptor compartment. To know the CYC amount diffused

through the membrane, the samples, after proper dilution with methanol, were analysed at 209 nm using a UV spectrophotometer. The experiments were conducted three times to achieve a consistent and precise average value.

2.5.6.8. Stability study. 60 ml HDPE bottles, each holding 40 capsules of CYC-SD-SSNEDSS and CYC-SE-S-SNEDDS (with each capsule containing 20 mg of cyclosporine), underwent accelerated testing under controlled conditions (40 ± 2 °C/75 ± 5% RH) using a stability chamber (Newtronic, India) for six months following sealing. At regular intervals during this timeframe, samples were taken from the bottles and assessed for changes in physical appearance, percentage cumulative drug release (% CDR), and disintegration time.[42] %CDR assessment used the same procedure and dissolution media described in the *In vitro* dissolution test section. The disintegration time was noted in the dissolution apparatus only when no residue of the capsule remained in the dissolution container (except for some fragments of the undissolved capsule).

3. Results and discussion

3.1. Drug solubility study

Many formulations face the issue of going through precipitation ahead of experiencing *in situ* solubilization, so for the confirmation of the formulation stability, the solubility of the drug in the excipients becomes vital. The high drug solubility in different excipients of the formulation remains the critical requirement for achieving maximum drug loading and bioavailability.[43] To develop an efficient L-SNEDDS of CYC, the recommended drug should be readily miscible in the chosen excipients with minimal incorporation into the mixture.[44] Fig. 1 shows the solubility of CYC in different excipients.

For proper self-emulsification to happen, the optimum mixture of excipients is required. Self-emulsification potential analysis revealed that Labrafac with the maximum amount of Capmul® GMS-50K was emulsified, as shown in Fig. 2.

Based on this observation, Capmul® GMS-50K and Labrafac were selected as an oil and surfactant, respectively. As shown in Table 1, with polyethylene glycol 400 (PEG 400), a wide range of nanoemulsion regions were observed compared with propylene glycol (PG). Therefore, it was used as a co-surfactant.

The high amounts of surfactant can enhance the self-emulsification phenomena. Using a co-surfactant does not interfere with surfactant properties to reduce the interfacial tension around the oily vehicle. The use of a co-surfactant reduces the

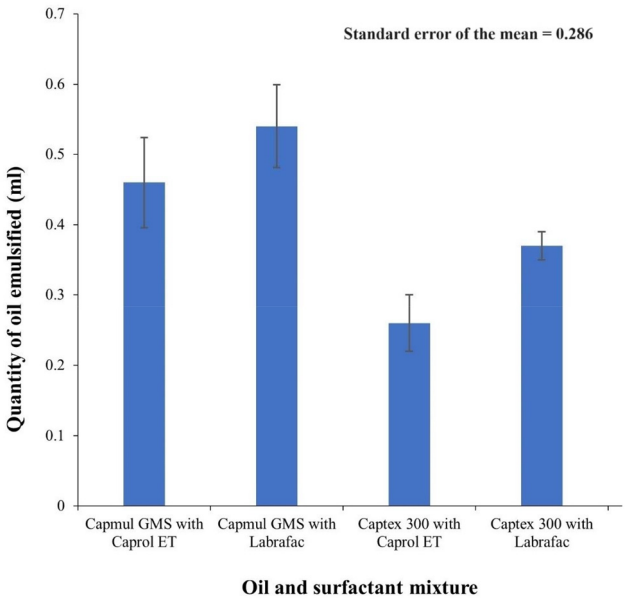

Fig. 2 Self-emulsification study (quantity of oil emulsified by the surfactants) (n = 3).

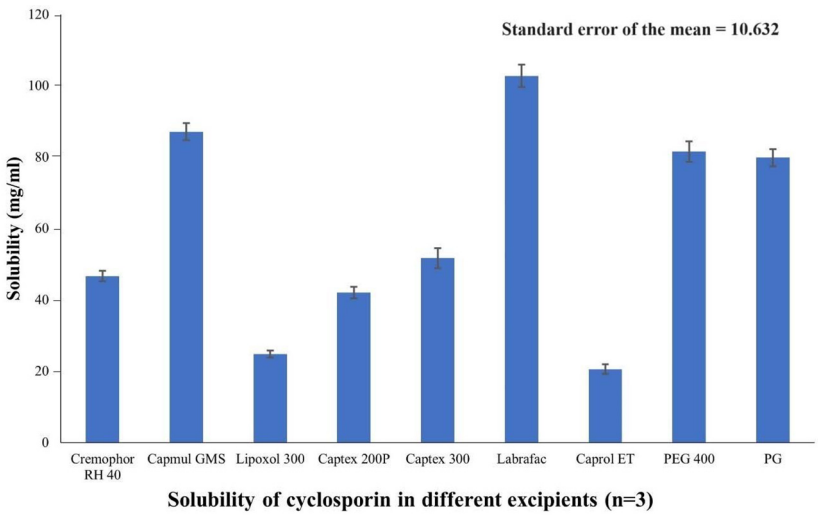

Fig. 1 Solubility of cyclosporin in different excipients (mg ml^{-1}).

Table 1 Nanoemulsion region formation (S_{mix} with different co-surfactants)

Composition		Nanoemulsion region	
Oil (%)	S_{mix} (%)	S_{mix} of Labrafac : PEG 400[a] (1 : 1)	S_{mix} of Labrafac : PG[a] (1 : 1)
10	90	Yes	Yes
20	80	Yes	Yes
30	70	Yes	Yes
40	60	Yes	Yes
50	50	Yes	No
60	40	Yes	No
70	30	No	No
80	20	No	No
90	10	No	No

[a] PEG 400 – polyethylene glycol 400, PG – propylene glycol.

amount of surfactant in the formulation.[45] PEG 400 is used as a co-surfactant in the formulation.

3.2. Pseudo-ternary phase diagram

To choose an appropriate ratio of excipients for L-SNEDDS and to observe the self-emulsification in the nano region, a pseudo-ternary phase diagram was plotted in the presence of CYC. The diagram helps to understand the phase behaviour of nanoemulsions.[46] The water-titration method was applied for plotting the diagram using an oily vehicle from 10–90% along with S_{mix} ratios (1 : 1, 1 : 2 and 2 : 1). As shown in Table 2, transparent regions were observed, which correspond to nanoemulsion regions and the pseudo ternary diagram was plotted using these data, where the shaded portion represents the transparent nanoemulsion (low viscosity) region shown in Fig. 3. Each apex part represents 100% of the excipient. S_{mix} (1 : 1) as a surfactant : co-surfactant mixture was found to be suitable.

3.3. Preparing the self-nanoemulsifying drug delivery system and solid-self-nanoemulsifying drug delivery system of cyclosporine

From the observations made through the pseudo ternary phase diagram, the composition of the oil, surfactant and co-surfactant was decided. As per the discussed method, the L-SNEDDS was formed and stored in an air-tight container. The final CYC-L-SNEDDS had a 100 mg of CYC, 400 mg of Capmul® GMS-50K, 300 mg of Labrafac and 300 mg of PEG 400 as a composition.

The microparticles developed by spray drying (SD-CHEM) and chitosan–EDTA microparticles by the solvent evaporation method (SE-CHEM) exhibited superior properties with high oil adsorption and desorption capacities and with favourable enhanced surface free energy components and dynamic advancing contact angles. The S-SNEDDS were developed independently, for both SD-CHEM and SE-CHEM, by adsorption or the solid carrier technique. Out of the two ratios of adsorbate (CYC-L-SNEDDS) : adsorbent (SD-CHEM), *i.e.* 1 : 1 and 1 : 1.5, the (1 : 1.5) ratio of the adsorbate (CYC-L-SNEDDS) : adsorbent

Table 2 Output of the water titration method with CYC, oil and S_{mix}

S. no.	% Oil	% Surfactant	% Co-surfactant	Appearance of resulted emulsion	Drug precipitation
S_{mix} ratio 1 : 1					
1.	10.0	45.0	45.0	Transparent	No
2.	20.0	40.0	40.0	Transparent	No
3.	30.0	35.0	35.0	Transparent	No
4.	40.0	30.0	30.0	Transparent/ bluish	No
5.	50.0	25.0	25.0	Transparent/ bluish	No
6.	60.0	20.0	20.0	Turbid	Yes
7.	70.0	15.0	15.0	Turbid	Yes
8.	80.0	10.0	10.0	Turbid	Yes
9.	90.0	5.0	5.0	Turbid	Yes
S_{mix} ratio 1 : 2					
1.	10.0	60.0	30.0	Transparent	No
2.	20.0	53.3	26.7	Transparent	No
3.	30.0	46.7	23.3	Transparent	No
4.	40.0	40.0	20.0	Transparent/ bluish	No
5.	50.0	33.3	16.7	Turbid	Yes
6.	60.0	26.7	13.3	Turbid	Yes
7.	70.0	20.0	10.0	Turbid	Yes
8.	80.0	13.3	6.7	Turbid	Yes
9.	90.0	6.7	3.3	Turbid	Yes
S_{mix} ratio 2 : 1					
1.	10.0	30.0	60.0	Turbid	Yes
2.	20.0	26.7	53.3	Transparent	No
3.	30.0	23.3	46.7	Transparent	No
4.	40.0	20.0	40.0	Transparent/ bluish	No
5.	50.0	16.7	33.3	Turbid	Yes
6.	60.0	13.3	26.7	Turbid	Yes
7.	70.0	10.0	20.0	Turbid	Yes
8.	80.0	6.7	13.3	Turbid	Yes
9.	90.0	3.3	6.7	Turbid	Yes

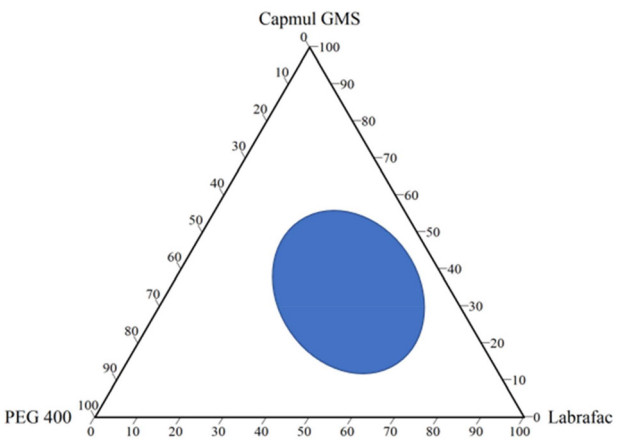

Fig. 3 Pseudo ternary phase diagram.

(SD-CHEM) was found to be non-sticky, free-flowing powder for CYC-SD-S-SNEDDS. For CYC-SE-S-SNEDDS, the two ratios of adsorbate (CYC-L-SNEDDS) : adsorbent (SE-CHEM), *i.e.* 1 : 1.5 and 1 : 2, the (1 : 2) ratio of the adsorbate (CYC-L-SNEDDS) : adsorbent (SE-CHEM) was found to be non-sticky and free-flowing powder. This adsorption technique especially

favours thermolabile drugs, where no heat treatment is given to the system. So, this drug's L-SNEDDS mixture (with the alcohol and adsorbent material) cannot be directly spray-dried because of the chances of drug degradation. Instead, spray-dried microparticles and the solvent-evaporated microparticles (without the drug) with superior adsorption properties were formed, and L-SNEDDS were adsorbed on them at lower temperatures. The resulting CYC-SD-S-SNEDDS, CYC-SE-S-SNEDDS, and CYC-L-SNEDDS were evaluated.

3.4. Evaluation of the CYC-L-SNEDDS, CYC-SD-S-SNEDDS and CYC-SE-S-SNEDDS

3.4.1. Drug loading efficiency. As mentioned in Table 3, the drug loading efficiencies of CYC-SD-S-SNEDDS and CYC-SE-S-SNEDDS were 81.18 ± 4.19% and 56.42 ± 5.47%, respectively. As expected, the drug loading efficiency (%) of CYC-L-SNEDDS was the highest *i.e.* 86.8 ± 4.86%. The CYC-SD-S-SNEDDS drug loading capacity was closer to that of CYC-L-SNEDDS, which proves the potential of SD-CHEM as superior microparticles. Unavoidable loss occurred in drug loading after solidification of CYC-L-SNEDDS to CYC-SD-S-SNEDDS and CYC-SE-S-SNEDDS by the adsorption technique.

3.4.2. Flow properties. For both CYC-SD-S-SNEDDS and CYC-SE-S-SNEDDS, the derived flow properties were calculated and are reported in Table 3. The bulk density of the CYC-SD-S-SNEDDS and CYC-SE-S-SNEDDS was 0.872 ± 0.113 g cm^{-3} and 0.699 ± 0.097 g cm^{-3}, respectively, which correspond to the presence of the gaps in between the powder particles and are significant for capsule filling operations in industry.[29] The tapped densities of the CYC-SD-S-SNEDDS and CYC-SE-S-SNEDDS were 0.914 ± 0.141 g cm^{-3} and 0.785 ± 0.154 g cm^{-3}, respectively. The minimal difference between both densities (bulk and tapped), Carr's index (CYC-SD-S-SNEDDS = 4.816 ± 0.026 and CYC-SE-S-SNEDDS = 12.446 ± 0.139), Hausner's ratio (CYC-SD-S-SNEDDS = 1.048 ± 0.065 and CYC-SE-S-SNEDDS = 1.124 ± 0.037) and the angle of repose (CYC-SD-S-SNEDDS = 16.263 ± 1.648 and CYC-SE-S-SNEDDS = 13.846 ± 1.426) signified the good flow properties for the formulations, which is a desired property during manufacturing in industry. Hence, SD-CHEM and SE-CHEM provided S-SNEDDS with a good flow.

3.4.3. Solid state characterisation

3.4.3.1. X-ray diffraction analysis. The identification of alterations in polymorphism, dissolution extent (solubility) and stability relies on the crucial quality attribute of particle crystallinity, as ascertained by XRD analysis. Fig. 4 shows an X-ray diffraction (XRD) analysis of CYC, SD-CHEM, CYC-SD-S-SNEDDS and CYC-SE-S-SNEDDS. CYC showed diffraction peaks at 2θ = 10.1°, 2θ = 12.5°, and 2θ = 28.5°. All these diffraction peaks correspond to the characteristic crystalline region

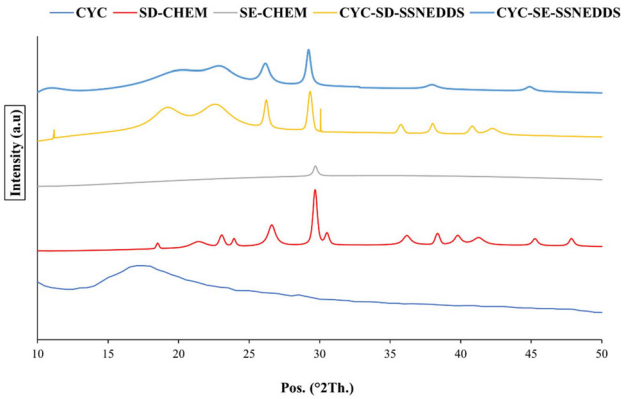

Fig. 4 XRD analysis of CYC, SD-CHEM, SE-CHEM, CYC-SD-S-SNEDDS and CYC-SE-S-SNEDDS.

Table 3 Flow properties, physical characterization, dissolution, and permeation profiles of the formulations

	CYC-L-SNEDDS	CYC-SD-S-SNEDDS	CYC-SE-S-SNEDDS
Flow properties			
Bulk density (g cm^{-3})	—	0.872 ± 0.113	0.699 ± 0.097
Tapped density (g cm^{-3})	—	0.914 ± 0.141	0.785 ± 0.154
Carr's Index (%)	—	4.816 ± 0.026	12.446 ± 0.139
Hausner's ratio	—	1.048 ± 0.065	1.124 ± 0.037
Angle of repose (θ)	—	16.263 ± 1.648	13.846 ± 1.426
Flowability	—	Excellent/good	Good/fair
Physical characterization			
Globule size (nm)	90.99 ± 2.81	138.7 ± 4.14	166.9 ± 4.04
PDI	0.618 ± 0.008	0.613 ± 0.004	0.579 ± 0.003
Zeta potential (mV)	−0.657 ± 0.392	−0.015 ± 0.057	−1.091 ± 0.937
Emulsification time (s)	18–22	34–37	45–49
Per cent transmittance	98.36 ± 0.181	93.87 ± 0.743	91.47 ± 1.032
Cloud temp. (°C)	71	58	55
Dissolution profiles			
Percent drug loading	86.812 ± 4.863	81.184 ± 4.191	56.426 ± 5.471
Dissolution efficiency (%)	82.116	80.039	72.267
Permeation profile			
Ex vivo permeation efficiency (%)	41.467	39.341	28.306
Flux	5.503	5.244	4.725
Permeability constant	1.101	1.048	0.945

Values are presented as mean ± standard deviation (S.D.), (n = 3).

of CYC.[47] The SD-CHEM samples showed diffraction peaks at 2θ = 18.51°, 2θ = 21.41°, 2θ = 26.61° and 2θ = 29.67°. Likewise, in SE-CHEM samples, the nearly vanishing diffraction peaks at 2θ = 21.2° and 2θ = 23°, along with the significantly broadened diffraction peaks at 2θ = 26.5° and 2θ = 29.8°, were observed. The CYC-SD-S-SNEDDS showed diffraction peaks at 2θ = 19.23°, 2θ = 22.7°, 2θ = 26.21° and 2θ = 29.33°, and diffraction peaks of the CYC-SE-S-SNEDDS were at 2θ = 20.31°, 2θ = 22.85°, 2θ = 26.15° and 2θ = 29.23°. As no distinctive characteristic peak of CYC is there in S-SNEDDS, it indicates amorphization of the CYC in the formulation. Consequently, beyond the benefits of self-emulsifying formulations, the improved dissolution behaviour anticipated from drug amorphization is attributed to nanometric sizes and the lack of crystallinity. The investigation further highlights the absence of any indications of CYC precipitation when incorporated into S-SNEDDS. Therefore, this proved the stability of the drug in the solid form, an advantage over the liquid form.

3.4.3.2. Surface morphology. To understand the shape and surface of the solid formulations, the SEM images of the SD-CHEM, SE-CHEM, CYC-SD-S-SNEDDS and CYC-SE-S-SNEDDS (shown in Fig. 5) were obtained. Fig. 5a shows the SD-CHEM, which is much spherical with uneven surfaces and large void spaces, leading to better oil adsorption and desorption. As shown in Fig. 5b, the SE-CHEM had a flaky appearance with an uneven surface, providing a high surface area for the adsorption of L-SNEDDS. Fig. 5c shows the CYC-SD-S-SNEDDS with a 5–8 μm size range. The adsorption with CYC-L-SNEDDS is visible with the smoothening of the uneven surfaces and void spaces, which were present in SD-CHEM. Similarly, in Fig. 5d, the CYC-SE-S-SNEDDS are visible with smooth, flaky structures compared to SE-CHEM and have a 10–12 μm size range. The good adsorption (of the L-SNEDDS) behaviour of microparticles (both SD-CHEM and SE-CHEM) is justified through SEM images, which indicated the small size of superior microparticles and high surface area.

3.4.4. FTIR analysis. The FTIR graphs are shown in Fig. 6. The Capmul® GMS-50K spectrum showed characteristic absorption bands at 1735 cm^{-1} (which corresponds to C═O), 1392–1216 cm^{-1} (attributable to CH_2 wagging vibrations), 1179 cm^{-1} (single peak attributed to C–O stretching approves stearate ester), and 720 cm^{-1} (points to aliphatic C–H bonds).[48] The Labrafac spectrum showed small sharp peaks at 2926 cm^{-1} and 2825 cm^{-1} corresponding to the CH_2 symmetric (stretching) vibrations and a peak at 1739 cm^{-1} confirming the ester group's C═O stretching vibrations. It also showed absorption at 1113 cm^{-1} and 722 cm^{-1}, corresponding to C–O groups and aliphatic C–H bonds.[49] PEG 400 showed absorption bands at 3391 cm^{-1} (corresponding to O–H stretching), 2873 cm^{-1} (confirming CH_2 groups with stretching vibrations), 1457 cm^{-1} (confirming CH_2 groups with bending vibrations), 1249 cm^{-1} (C–O stretching vibrations) and 948 cm^{-1} (confirming C–O–C stretching).[50] SE-CHEM and SD-CHEM exhibited absorption bands in the range of 1676–1657 cm^{-1} and 1693–1667 cm^{-1}, respectively, indicative of the presence of the amide linkage. They also showed absorption bands between 2378 cm^{-1} and 2373 cm^{-1}, suggesting free acetate moieties. This indicates that not all acetate moieties are involved in the amide linkage. The FTIR spectra of CYC showed the band at 3306 cm^{-1}, confirming primary and secondary amines (N–H stretching

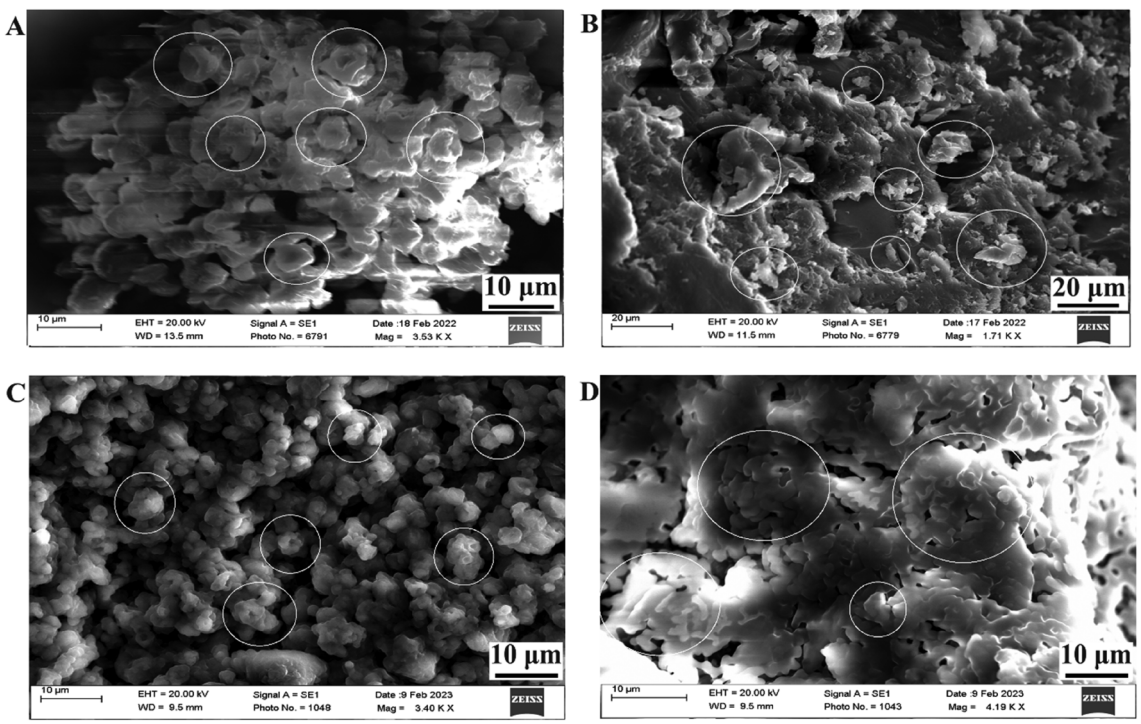

Fig. 5 Surface morphology of (A) SD-CHEM, (B) SE-CHEM, (C) CYC-SD-S-SNEDDS and (D) CYC-SE-S-SNEDDS.

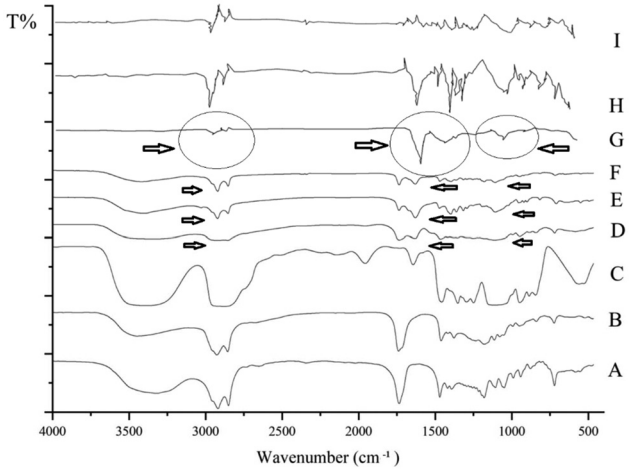

Fig. 6 FTIR spectra of (A) Capmul GMS, (B) Labrafac, (C) PEG 400, (D) CYC-L-SNEDDS, (E) CYC-SD-S-SNEDDS, (F) CYC-SE-S-SNEDDS, (G) CYC, (H) SD-CHEM and (I) SE-CHEM.

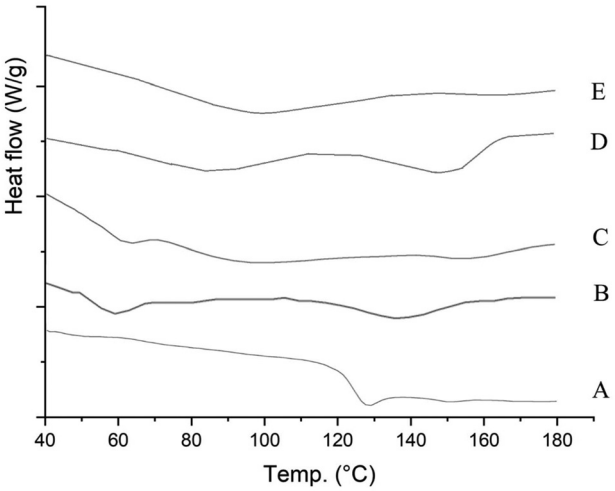

Fig. 7 DSC curves of (A) CYC, (B) CYC-SD-S-SNEDDS, (C) CYC-SE-S-SNEDDS, (D) SD-CHEM, and (E) SE-CHEM.

vibrations). The 2966–2877 cm^{-1} absorption band corresponds to alkyl groups (C–H stretching vibrations). The absorption bands at 1625 cm^{-1} and 1095 cm^{-1} confirmed the amide group (C═O stretching vibration) and C–O stretching vibrations, respectively.[51,52] No significant changes were observed in the spectra of CYC-L-SNEDDS, CYC-SD-S-SNEDDS and CYC-SE-S-SNEDDS regarding the characteristic peak of the CYC. The CYC-L-SNEDDS spectra showed absorptions at 3321 cm^{-1}, 2922 cm^{-1}, 2855 cm^{-1}, 1631 cm^{-1}, 1466 cm^{-1} and 1110 cm^{-1}. The CYC-SD-S-SNEDDS spectra showed absorptions at 3403 cm^{-1}, 2922 cm^{-1}, 2854 cm^{-1}, 1629 cm^{-1}, 1472 cm^{-1} and 1107 cm^{-1}. The CYC-SE-S-SNEDDS spectra showed absorptions at 3418 cm^{-1}, 2921 cm^{-1}, 2853 cm^{-1}, 1630 cm^{-1}, 1469 cm^{-1} and 1107 cm^{-1}. The broadening of some peaks and a negligible shift in peaks were observed, possibly due to hydrogen bonds between drugs and surfactants.[53]

3.4.5. DSC analysis. DSC analysis was used to observe any polymorphic changes by using drugs and excipients. The thermograms of the CYC, CYC-SD-S-SNEDDS and CYC-SE-S-SNEDDS, SD-CHEM and SE-CHEM were obtained and are shown in Fig. 7. The characteristic endothermic peak of the CYC was observed at 128 °C. In CYC-SD-S-SNEDDS, the endothermic peak disappeared, and a broad bulge was observed near 140 °C. A similar broad peak was observed in CYC-SE-S-SNEDDS near 100 °C. This may be due to the physical dispersion of the CYC with excipients, as reported earlier.[54,55] The thermograms of CYC-SD-S-SNEDDS and CYC-SE-S-SNEDDS exhibited a broad endothermic peak around 60 °C, which is attributed to the evaporation of moisture or the presence of acetic acid moieties (which was used during the preparation of the CH : EDTA microparticles, *i.e.* SD-CHEM and SE-CHEM).[28]

3.4.6. Evaluation of the reconstituted nanoemulsion and CYC-L-SNEDDS

3.4.6.1. Determination of the globule size, size distribution and zeta potential. The globule size determination is a crucial factor in determining the self-nanoemulsification property of the system. Based on this, the degree of drug release and absorption can be estimated, as a small globule size in the nanometric range can lead to a greater surface area (interfacial) and better drug absorption. In Table 3, the globule sizes (and polydispersity index, PDI) of the CYC-L-SNEDDS, CYC-SD-S-SNEDDS, and CYC-SE-S-SNEDDS are 90.0 nm (PDI: 0.618), 138.7 (PDI: 0.613), and 166.9 (PDI: 0.579). From the results, it is clear that the globule size (nm) of the CYC-SD-S-SNEDDS is close to that of the CYC-L-SNEDDS, whereas CYC-SE-S-SNEDDS had a considerable difference. The PDI of all the formulations was very close to each other. So, the small globule size and PDI were observed from both SD-CHEM and SE-CHEM surfaces. SD-CHEM (CYC-SD-S-SNEDDS), as an adsorbent, was better than SE-CHEM in producing small-sized globules and high PDI. The zeta potential results for CYC-L-SNEDDS, CYC-SD-S-SNEDDS, and CYC-SE-S-SNEDDS were −0.657 mV, −0.015 mV, and −1.09 mV, respectively. The results of the S-SNEDDS were very close to those of L-SNEDDS. S-SNEDDS are comparatively more stable than L-SNEDDS and reconstitution to nanoemulsion in the former only happens inside the body, so there are negligible chances of agglomeration during the shelf-life of the formulation.

3.4.6.2. Self-emulsification time. As reported in Table 3, the emulsification time for CYC-L-SNEDDS, CYC-SD-S-SNEDDS and CYC-SE-S-SNEDDS was 18–22, 34–37, and 45–49 seconds, respectively. This shows that all systems had the ability to disperse immediately under aqueous conditions under agitation, which signifies the rapid dispersion ability of S-SNEDDS after reconstitution.

3.4.6.3. Percent transmittance test. The results of the percent transmittance for CYC-L-SNEDDS, CYC-SD-S-SNEDDS, and CYC-SE-S-SNEDDS are shown in Table 3 and were greater than 90%, which proves the efficacy of self-emulsification. This transparency also confirms the stability of the reconsti-

tuted nanoemulsion and negates the chances of drug precipitation.[56]

3.4.6.4. Cloud point estimation. The cloud point temperature is the temperature where the transparent nature of the SNEDDS changes to cloudy or turbid (change in phase behaviour). It should be above the temperature at which SNEDDS will be used, usually 37 °C. All the values of the cloud point temperatures for CYC-L-SNEDDS, CYC-SD-S-SNEDSS and CYC-SE-S-SNEDDS were above 37 °C, thus confirming the thermodynamic stability[57] of the formulations after reconstitution.

3.4.6.5. Field emission scanning electron microscopy. Fig. 8(a and b) show the FE-SEM images of CYC-SD-S-SNEDDS and Fig. 8(c and d) show the images of CYC-SE-S-SNEDDS. It is evident from the images that all the reconstituted globules obtained from both the S-SNEDDS were spherical. These images also confirm the size analysed using the Zetasizer (mentioned in Table 3). The globules formed were fine in size, and no coalescence was observed, suggesting the stability of reconstituted nanoemulsions. The small globule size will determine the ability of the reconstituted SNEDDS to get absorbed and its diffusion from the biological membranes.

3.4.6.6. In vitro dissolution study. The *in vitro* dissolution study was performed for pure CYC, CYC-L-SNEDDS, CYC-SD-S-SNEDDS, and CYC-SE-S-SNEDDS and the graph of percent cumulative drug release (%CDR) for all is shown in Fig. 9. After 30 minutes of the study, the %CDR values for pure CYC, CYC-L-SNEDDS, CYC-SD-S-SNEDDS, and CYC-SE-S-SNEDSS

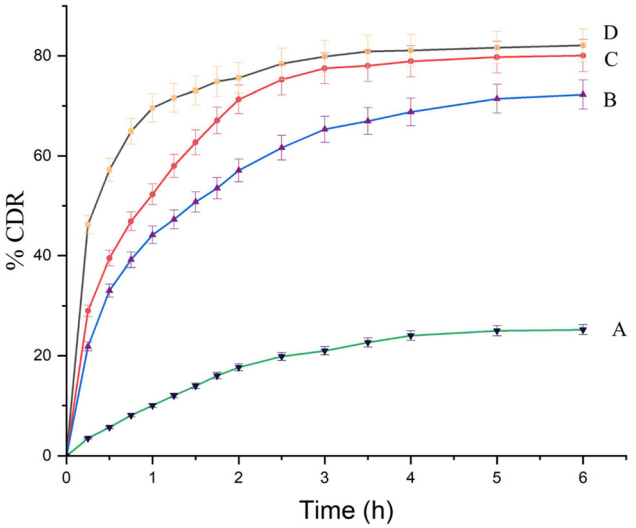

Fig. 9 Dissolution profile (% cumulative drug release) of (A) CYC (B) CYC-SE-S-SNEDDS, (C) CYC-SD-S-SNEDDS and (D) CYC-L-SNEDDS (n = 3).

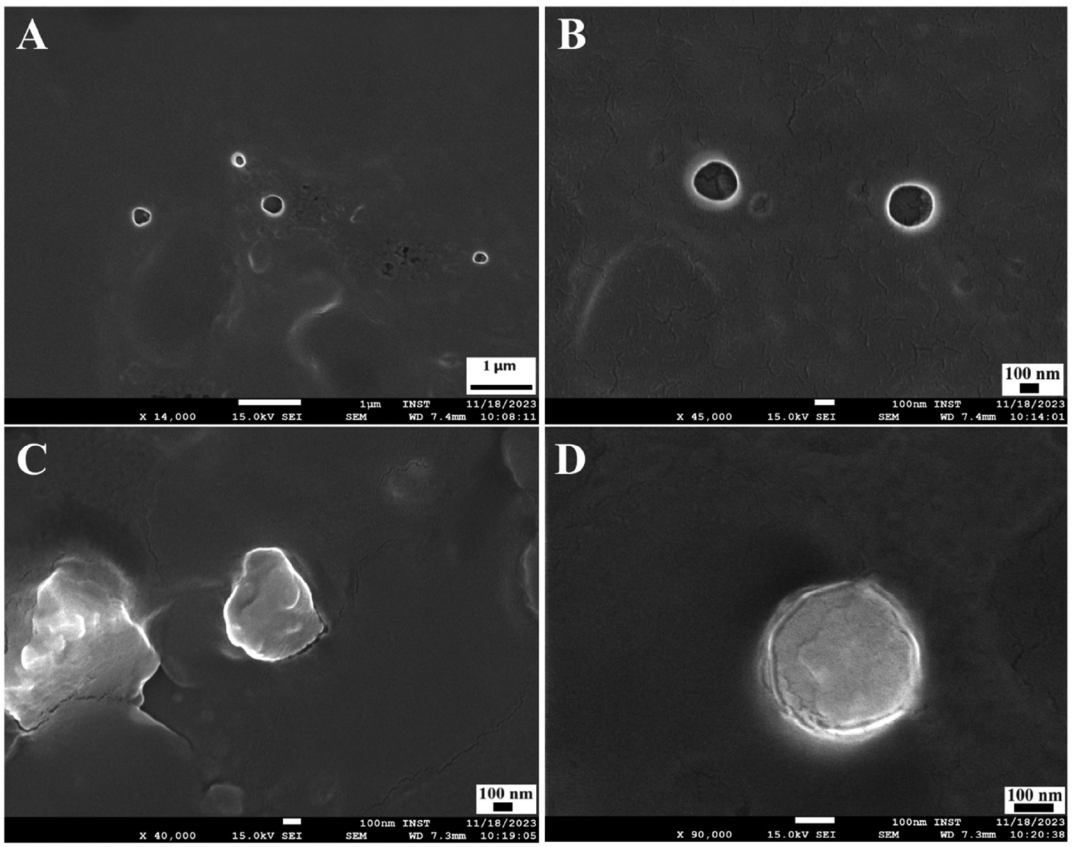

Fig. 8 FE-SEM images (at different magnifications) of (A) and (B) CYC-SD-S-SNEDDS, and (C) and (D) CYC-SE-S-SNEDDS.

were 57.18%, 39.51%, 33.01% and 5.63%, respectively. The highest %CDR in CYC-L-SNEDDS in a short time was obvious because of its liquid nature. While in CYC-SD-S-SNEDDS and CYC-SE-S-SNEDDS, the drug (in SNEDDS on solid adsorbents) had taken a little more time to get desorbed from the surface of the solid and emulsify and dissolute. An 8-fold and 7-fold increase in drug dissolution of CYC was observed in CYC-SD-S-SNEDDS and CYC-SE-S-SNEDDS, respectively, compared to the pure CYC. The final release of the drug from the L-SNEDDS and S-SNEDDS was quite close to each other, especially if we compare CYC-L-SNEDDS and CYC-SD-S-SNEDDS were significantly closer, which proves the facilitation of CYC dissolution with these S-SNEDDS.

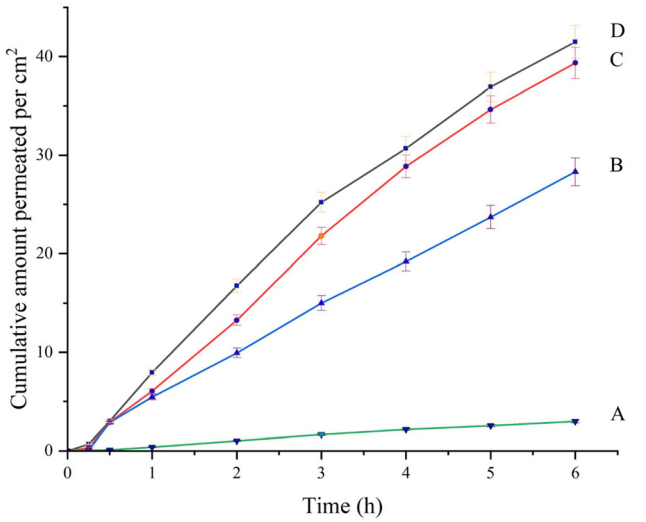

Fig. 10 *Ex vivo* permeation profile of (A) CYC (B) CYC-SE-S-SNEDDS, (C) CYC-SD-S-SNEDDS and (D) CYC-L-SNEDDS (n = 3).

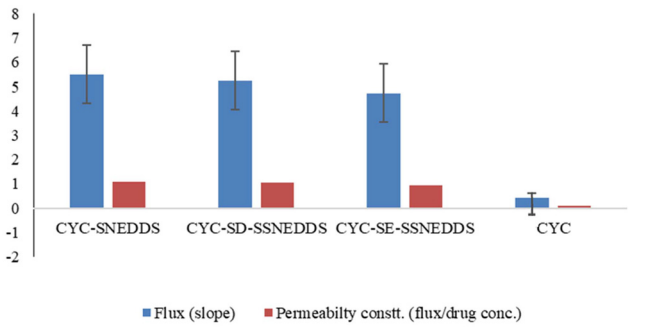

Fig. 11 *Ex vivo* permeation parameters of CYC, CYC-SE-S-SNEDDS, CYC-SD-S-SNEDDS and CYC-L-SNEDDS (n = 3).

3.4.6.7. Ex vivo permeation study. This study was performed to know the permeability of the drug through a biological membrane (diffusion barrier), and it was compared for pure CYC, CYC-L-SNEDDS, reconstituted CYC-SD-S-SNEDDS, and CYC-SE-S-SNEDSS. Fig. 10 shows the results of the cumulative amount permeated per cm^2 and showed that all the formulations had increased the permeation of the drug to many folds as compared with pure CYC. According to the results, the CYC-L-SNEDDS, reconstituted CYC-SD-S-SNEDDS, and CYC-SE-S-SNEDDS had permeation of 41.467%, 39.341% and 28.306%, respectively, which is significantly closer for both CYC-L-SNEDDS and reconstituted CYC-SD-S-SNEDDS. Fig. 11 shows the flux and permeability constant. Flux is the amount of drug permeated per unit area per unit time through a diffusion barrier (μg min^{-1} cm^{-2}) × 10^{-2} (slope of the permeability curve). Permeability constant defines the ease of drug diffusion from the permeable membrane (flux/drug conc.) The results suggested that the permeability behaviour of the cumulative amount of drug released from the CYC-L-SNEDDS and CYC-SD-S-SNEDDS was considerably closer, and the difference was 0.054% and 0.464%, respectively. The permeability constant and flux of the CYC-L-SNEDDS, CYC-SD-S-SNEDDS and CYC-SE-S-SNEDDS were significantly close to each other, which suggests that the diffusion profile of the drug (across the biological membrane) in both liquid and solid formulations is almost similar. These results indicated that both CYC-SD-S-SNEDDS and CYC-SE-S-SNEDDS could produce nanosized globules of the nanoemulsion with the drug, which can diffuse from the biological membrane and successfully transport the drug in a similar manner to the L-SNEDDS.

Table 4 Stability study data for cyclosporine formulations (CYC-SD-S-SNEDDS and CYC-SE-S-SNEDDS)

Formulation	Parameters	Initial	1 month (40 ± 2 °C/75 ± 5% RH)	3 months (40 ± 2 °C/75 ± 5% RH)	6 months (40 ± 2 °C/75 ± 5% RH)
CYC-SD-S-SNEDDS	Description	Whitish colored capsules with S-SNEDDS	Whitish colored capsules with S-SNEDDS	Whitish colored capsules with S-SNEDDS	Whitish colored capsules with S-SNEDDS
	%CDR	80.0% ± 3.2	79.08% ± 1.1	80.12% ± 2.7	81.19% ± 0.8
	Disintegration time (min)	5 ± 1.6	5 ± 2.1	6 ± 0.9	6 ± 1.5
CYC-SE-S-SNEDDS	Description	Whitish colored capsules with S-SNEDDS	Whitish colored capsules with S-SNEDDS	Whitish colored capsules with S-SNEDDS	Whitish colored capsules with S-SNEDDS
	%CDR	72.3% ± 2.9	72.43% ± 1.4	71.74% ± 2.1	71.13% ± 2.1
	Disintegration time (min)	6 ± 0.5	6 ± 1.8	7 ± 1.3	7 ± 1.6

3.4.6.8 Stability study. The summarized findings from the stability investigation are depicted in Table 4. Evaluation of the data demonstrated that both CYC-SD-S-SNEDDS and CYC-SE-S-SNEDDS maintained stability over the six-month accelerated testing period at 40 ± 2 °C/75 ± 5% RH and when reconstituted into nanoemulsions after one, three and six months, no significant difference was observed in color, form, %CDR and disintegration time. Consequently, it can be inferred that both CYC-SD-S-SNEDDS and CYC-SE-S-SNEDDS formulations have satisfactorily met the stability criteria (Table 4).

4. Conclusion

Solid self-nanoemulsifying drug delivery systems of cyclosporine were successfully developed by using Capmul® GMS-50K, Labrafac and PEG 400 as the oil, surfactant, and co-surfactant, respectively. These ingredients were selected on the basis of different analyses like solubility studies and self-emulsification potential analysis. After observing a suitable ratio for self-nanoemulsification through a pseudo ternary phase diagram, the self-nanoemulsifying drug delivery system was developed with a final ratio of oil and S_{mix} [surfactant : co-surfactant (1 : 1)] as 40 : 60. SD-CHEM and SE-CHEM microparticles developed through spray drying and solvent evaporation methods, respectively, were used as adsorbents to form S-SNEDDS of cyclosporine, *i.e.* CYC-SD-S-SNEDDS and CYC-SE-S-SNEDDS, respectively. In both these formulations, the liquid CYC-L-SNEDDS was used as an adsorbate. The final ratio of adsorbate : adsorbent for CYC-SD-S-SNEDDS and CYC-SE-S-SNEDDS was 1 : 1.5 and 1 : 2, respectively. Both formulations exhibited good drug loading and excellent flow properties. X-ray diffractograms revealed that the drug was present in an amorphous state in both preparations. Scanning electron micrographs revealed even adsorption of L-SNEDDS over solid microparticles. The FTIR and DSC analyses confirmed no interactions between different drugs and excipients. The nanometric size of globules with the smallest PDIs was observed for both the S-SNEDDS. The stability study and FE-SEM images confirmed the physical and thermodynamic stability of the reconstituted nanoemulsions from both the S-SNEDDS. The *in vitro* dissolution study showed an 8-fold and 7-fold increase in drug dissolution compared to the pure drug and dissolution profiles of S-SNEDDS were quite closer to those of the L-SNEDDS. Furthermore, an *in vivo* study can be carried out to establish the relationship between the dissolution, permeation and bioavailability profiles of S-SNEDDS.

Abbreviations

CYC	Cyclosporine
BCS	Biopharmaceutical classification system
SNEDDS	Self-nanoemulsifying drug delivery system
L-SNEDDS	Liquid self-nanoemulsifying drug delivery system
GIT	Gastrointestinal tract
S-SNEDDS	Solid self-nanoemulsifying drug delivery systems
CYC-L-SNEDDS	Liquid self-nanoemulsifying nano drug delivery system of the cyclosporine
SD-CHEM	Spray dried chitosan–EDTA microparticles
SE-CHEM	Solvent evaporated chitosan–EDTA microparticles
CYC-SD-S-SNEDDS	Cyclosporine solid self-nanoemulsifying drug delivery system with spray dried microparticles
CYC-SE-S-SNEDDS	Cyclosporine solid self-nanoemulsifying drug delivery system with solvent evaporated microparticles
XRD	X-ray diffraction
SEM	Scanning electron microscopy
FTIR	Fourier-transform infrared spectroscopy analysis
DSC	Differential scanning calorimetry
FE-SEM	Field emission scanning electron microscopy
PDI	Polydispersibity index
%CDR	%cumulative drug release

Data availability

The data shall be made available on demand. The ESI† is also attached on the submission portal.

Conflicts of interest

There are no conflicts to declare.

References

1 H. F. Stähelin, The history of cyclosporin A (Sandimmune®) revisited: Another point of view, *Experientia*, 1996, **52**, 5–13.
2 M. Guada, A. Beloqui, M. N. V. R. Kumar, V. Préat, M. D. C. Dios-Viéitez and M. J. Blanco-Prieto, Reformulating cyclosporine A (CsA): More than just a life cycle management strategy, *J. Controlled Release*, 2016, **225**, 269–282.
3 C. J. Dunn, A. J. Wagstaff, C. M. Perry, G. L. Plosker and K. L. Goa, Cyclosporin: An Updated Review of the Pharmacokinetic Properties, Clinical Efficacy and Tolerability of a Microemulsion-Based Formulation (Neoral)* in Organ Transplantation, *Drugs*, 2001, **61**, 1957–2016.
4 S. A. Survase, L. D. Kagliwal, U. S. Annapure and R. S. Singhal, Cyclosporin A—A review on fermentative production, downstream processing and pharmacological applications, *Biotechnol. Adv.*, 2011, **29**, 418–435.
5 P. Berton, M. K. Mishra, H. Choudhary, A. S. Myerson and R. D. Rogers, Solubility Studies of Cyclosporine Using Ionic Liquids, *ACS Omega*, 2019, **4**, 7938–7943.

6 G. L. Amidon, H. Lennernäs, V. P. Shah and J. R. Crison, A theoretical basis for a biopharmaceutic drug classification: the correlation of in vitro drug product dissolution and in vivo bioavailability, *Pharm. Res.*, 1995, **12**, 413–420.
7 Y.-Y. Chiu, Human Jejunal Permeability of Cyclosporin A: Influence of Surfactants on P-Glycoprotein Efflux in Caco-2 Cells, *Pharm. Res.*, 2003, **20**, 749–756.
8 U. Christians and K.-F. Sewing, Cyclosporin metabolism in transplant patients, *Pharmacol. Ther.*, 1993, **57**, 291–345.
9 M. S. Flippin, C. E. Canter and D. T. Balzer, Increased morbidity and high variability of cyclosporine levels in pediatric heart transplant recipients, *J. Heart. Lung Transplant.*, 2000, **19**, 343–349.
10 R. Neslihan Gursoy and S. Benita, Self-emulsifying drug delivery systems (SEDDS) for improved oral delivery of lipophilic drugs, *Biomed. Pharmacother.*, 2004, **58**, 173–182.
11 Z. Yujin, Y. Jing and Z. Quan, Self-emulsifying drug delivery system improve oral bioavailability: role of excipients and physico-chemical characterization, *Pharm. Nanotechnol.*, 2020, **8**, 290–301.
12 E. K. G. Mhango, B. R. Sveinbjornsson, B. S. Snorradottir and S. Gizurarson, Incompatibility of antimalarial drugs: challenges in formulating combination products for malaria, *Drug Delivery*, 2024, **31**, 2299594.
13 M. C. Tekeli, Y. Aktas and N. Celebi, Oral self-nanoemulsifying formulation of GLP-1 agonist peptide exendin-4: development, characterization and permeability assesment on Caco-2 cell monolayer, *Amino Acids*, 2021, **53**, 73–88.
14 D. H. Truong, T. H. Tran, T. Ramasamy, J. Y. Choi, H. H. Lee, C. Moon, H.-G. Choi, C. S. Yong and J. O. Kim, Development of solid self-emulsifying formulation for improving the oral bioavailability of erlotinib, *AAPS PharmSciTech*, 2016, **17**, 466–473.
15 X. Yang, W. Li, S. Li, S. Chen, Z. Hu, Z. He, X. Zhu, X. Niu, X. Zhou, H. Li, Y. Xiao, J. Liu, X. Sui, G. Chen and Y. Gao, Fish oil-based microemulsion can efficiently deliver oral peptide blocking PD-1/PD-L1 and simultaneously induce ferroptosis for cancer immunotherapy, *J. Controlled Release*, 2024, **365**, 654–667.
16 V. Jannin, J. Musakhanian and D. Marchaud, Approaches for the development of solid and semi-solid lipid-based formulations, *Adv. Drug Delivery Rev.*, 2008, **60**, 734–746.
17 D. H. Oh, J. H. Kang, D. W. Kim, B.-J. Lee, J. O. Kim, C. S. Yong and H.-G. Choi, Comparison of solid self-microemulsifying drug delivery system (solid SMEDDS) prepared with hydrophilic and hydrophobic solid carrier, *Int. J. Pharm.*, 2011, **420**, 412–418.
18 J. D. Friedl, A. M. Jörgensen, B. Le-Vinh, D. E. Braun, M. Tribus and A. Bernkop-Schnürch, Solidification of self-emulsifying drug delivery systems (SEDDS): Impact on storage stability of a therapeutic protein, *J. Colloid Interface Sci.*, 2021, **584**, 684–697.
19 V. Garg, P. Kaur, S. K. Singh, B. Kumar, P. Bawa, M. Gulati and A. K. Yadav, Solid self-nanoemulsifying drug delivery systems for oral delivery of polypeptide-k: formulation, optimization, *in vitro* and *in vivo* antidiabetic evaluation, *Eur. J. Pharm. Sci.*, 2017, **109**, 297–315.
20 Y. G. Seo, D.-W. Kim, K. H. Cho, A. M. Yousaf, D. S. Kim, J. H. Kim, J. O. Kim, C. S. Yong and H.-G. Choi, Preparation and pharmaceutical evaluation of new tacrolimus-loaded solid self-emulsifying drug delivery system, *Arch. Pharmacal Res.*, 2015, **38**, 223–228.
21 M. Kumar, P. A. Chawla, A. Faruk and V. Chawla, Spray Drying as an Effective Method in the Development of Solid Self- Emulsifying Drug Delivery Systems, *Curr. Drug Delivery*, 2023, **20**, 508–525.
22 A. Sirvi, K. Kuche, D. Chaudhari, R. Ghadi, T. Date, S. S. Katiyar and S. Jain, Supersaturable self-emulsifying drug delivery system: A strategy for improving the loading and oral bioavailability of quercetin, *J. Drug Delivery Sci. Technol.*, 2022, **71**, 103289.
23 H. N. ElShagea, N. A. ElKasabgy, R. H. Fahmy and E. B. Basalious, Freeze-Dried Self-Nanoemulsifying Self-Nanosuspension (SNESNS): a New Approach for the Preparation of a Highly Drug-Loaded Dosage Form, *AAPS PharmSciTech*, 2019, **20**, 258.
24 R. Verma, V. Mittal and D. Kaushik, Quality Based Design Approach for Improving Oral Bioavailability of Valsartan Loaded Smedds And Study of Impact of Lipolysis on the Drug Diffusion, *Drug Delivery Lett.*, 2018, **8**, 130–139.
25 J.-H. Lee, H. Kim, Y. Cho, T.-S. Koo and G. Lee, Development and Evaluation of Raloxifene-Hydrochloride-Loaded Supersaturatable SMEDDS Containing an Acidifier, *Pharmaceutics*, 2018, **10**, 78.
26 R. Verma and D. Kaushik, Design and optimization of candesartan loaded self-nanoemulsifying drug delivery system for improving its dissolution rate and pharmacodynamic potential, *Drug Delivery*, 2020, **27**, 756–771.
27 A. B. Mohd, K. Sanka, S. Bandi, P. V. Diwan and N. Shastri, Solid self-nanoemulsifying drug delivery system (S-SNEDDS) for oral delivery of glimepiride: development and antidiabetic activity in albino rabbits, *Drug Delivery*, 2015, **22**, 499–508.
28 M. Kumar, P. A. Chawla, A. Faruk, V. Chawla, S. Thakur and S. K. Jain, Development of superior chitosan–EDTA microparticles as an adsorbent base for solidifying the self-emulsifying drug delivery systems, *Future J. Pharm. Sci.*, 2024, **10**, 18.
29 S. Verma, S. K. Singh and P. R. P. Verma, Solidified SNEDDS of loratadine: formulation using hydrophilic and hydrophobic grades of Aerosil®, pharmacokinetic evaluations and in vivo–in silico predictions using GastroPlusTM, *RSC Adv.*, 2016, **6**, 3099–3116.
30 M. Dixit, A. G. Kini and P. K. Kulkarni, Preparation and characterization of microparticles of piroxicam by spray drying and spray chilling methods, *Res. Pharm. Sci.*, 2010, **5**, 89–97.
31 G. Shazly and K. Mohsin, Dissolution improvement of solid self-emulsifying drug delivery systems of fenofi brate using an inorganic high surface adsorption material, *Acta Pharm.*, 2015, **65**, 29–42.

32 F. H. Blindheim and J. Ruwoldt, The Effect of Sample Preparation Techniques on Lignin Fourier Transform Infrared Spectroscopy, *Polymers*, 2023, **15**, 2901.
33 S. P. Bang, C. Y. Yeon, N. Adhikari, S. Neupane, H. Kim, D. C. Lee, M. J. Son, H. G. Lee, J.-Y. Kim and J. H. Jun, Cyclosporine A eyedrops with self-nanoemulsifying drug delivery systems have improved physicochemical properties and efficacy against dry eye disease in a murine dry eye model, *PLoS One*, 2019, **14**, e0224805.
34 C. Rathore, C. Hemrajani, A. K. Sharma, P. K. Gupta, N. K. Jha, A. A. A. Aljabali, G. Gupta, S. K. Singh, J.-C. Yang, R. P. Dwivedi, K. Dua, D. K. Chellappan, P. Negi and M. M. Tambuwala, Self-nanoemulsifying drug delivery system (SNEDDS) mediated improved oral bioavailability of thymoquinone: optimization, characterization, pharmacokinetic, and hepatotoxicity studies, *Drug Delivery Transl. Res.*, 2023, **13**, 292–307.
35 N. Rangaraj, S. Shah, A. J. Maruthi, S. R. Pailla, H. S. Cheruvu, D. Sujatha and S. Sampathi, Quality by Design Approach for the Development of Self-Emulsifying Systems for Oral Delivery of Febuxostat: Pharmacokinetic and Pharmacodynamic Evaluation, *AAPS PharmSciTech*, 2019, **20**, 267.
36 S. Beg, O. P. Katare, S. Saini, B. Garg, R. K. Khurana and B. Singh, Solid self-nanoemulsifying systems of olmesartan medoxomil: formulation development, micromeritic characterization, in vitro and in vivo evaluation, *Powder Technol.*, 2016, **294**, 93–104.
37 S. Beg, S. S. Jena, C. N. Patra, M. Rizwan, S. Swain, J. Sruti, M. E. B. Rao and B. Singh, Development of solid self-nanoemulsifying granules (SSNEGs) of ondansetron hydrochloride with enhanced bioavailability potential, *Colloids Surf., B*, 2013, **101**, 414–423.
38 S. Bandyopadhyay, O. P. Katare and B. Singh, Optimized self nano-emulsifying systems of ezetimibe with enhanced bioavailability potential using long chain and medium chain triglycerides, *Colloids Surf., B*, 2012, **100**, 50–61.
39 A. K. Janakiraman, T. Islam, K. B. Liew, M. Elumalai and J. C. Hanish Singh, Improved oral bioavailability of poorly water-soluble vorinostat by self-microemulsifying drug delivery system, *Beni-Suef Univ. J. Basic Appl. Sci.*, 2022, **11**, 99.
40 A. Hussain, S. Kumar Singh, P. Ranjan Prasad Verma, N. Singh and F. Jalees Ahmad, Experimental design-based optimization of lipid nanocarrier as delivery system against *Mycobacterium* species: *in vitro* and *in vivo* evaluation, *Pharm. Dev. Technol.*, 2017, **22**, 910–927.
41 K. Singh, A. K. Tiwary and V. Rana, Spray dried chitosan–EDTA superior microparticles as solid substrate for the oral delivery of amphotericin B, *Int. J. Biol. Macromol.*, 2013, **58**, 310–319.
42 M. N. Mohd Izham, Y. Hussin, M. N. M. Aziz, S. K. Yeap, H. S. Rahman, M. J. Masarudin, N. E. Mohamad, R. Abdullah and N. B. Alitheen, Preparation and Characterization of Self Nano-Emulsifying Drug Delivery System Loaded with Citraland Its Antiproliferative Effect on Colorectal Cells In Vitro, *Nanomaterials*, 2019, **9**, 1028.
43 N. Parmar, N. Singla, S. Amin and K. Kohli, Study of cosurfactant effect on nanoemulsifying area and development of lercanidipine loaded (SNEDDS) self nanoemulsifying drug delivery system, *Colloids Surf., B*, 2011, **86**, 327–338.
44 X. Qi, L. Wang, J. Zhu, Z. Hu and J. Zhang, Self-double-emulsifying drug delivery system (SDEDDS): A new way for oral delivery of drugs with high solubility and low permeability, *Int. J. Pharm.*, 2011, **409**, 245–251.
45 P. R. Nepal, H.-K. Han and H.-K. Choi, Preparation and in vitro–in vivo evaluation of Witepsol® H35 based self-nanoemulsifying drug delivery systems (SNEDDS) of coenzyme Q10, *Eur. J. Pharm. Sci.*, 2010, **39**, 224–232.
46 K. Balakumar, C. V. Raghavan, N. T. Selvan, R. H. Prasad and S. Abdu, Self nanoemulsifying drug delivery system (SNEDDS) of Rosuvastatin calcium: Design, formulation, bioavailability and pharmacokinetic evaluation, *Colloids Surf., B*, 2013, **112**, 337–343.
47 S. Mirzaeei, G. Mohammadi, N. Fattahi, P. Mohammadi, A. Fattahi, M. R. Nikbakht and K. Adibkia, Formulation and Physicochemical Characterization of Cyclosporine Microfiber by Electrospinning, *Adv. Pharm. Bull.*, 2019, **9**, 249–254.
48 S. Kumar and J. K. Randhawa, Paliperidone-loaded spherical solid lipid nanoparticles, *RSC Adv.*, 2014, **4**, 30186–30192.
49 A. Kiani, M. Fathi and S. M. Ghasemi, Production of novel vitamin D $_3$ loaded lipid nanocapsules for milk fortification, *Int. J. Food Prop.*, 2017, **20**, 2466–2476.
50 M. Sahu, V. R. M. Reddy, B. Kim, B. Patro, C. Park, W. K. Kim and P. Sharma, Fabrication of Cu2ZnSnS4 Light Absorber Using a Cost-Effective Mechanochemical Method for Photovoltaic Applications, *Materials*, 2022, **15**, 1708.
51 P. Dubey, S. A. Barker and D. Q. M. Craig, Design and Characterization of Cyclosporine A-Loaded Nanofibers for Enhanced Drug Dissolution, *ACS Omega*, 2020, **5**, 1003–1013.
52 X. Jiang, Y. Zhao, Q. Guan, S. Xiao, W. Dong, S. Lian, H. Zhang, M. Liu, Z. Wang and J. Han, Amorphous solid dispersions of cyclosporine A with improved bioavailability prepared via hot melt extrusion: Formulation, physicochemical characterization, and in vivo evaluation, *Eur. J. Pharm. Sci.*, 2022, **168**, 106036.
53 J. B. Saliba, A. D. Silva-Cunha Junior, G. R. D. Silva, M. I. Yoshida, A. A. P. Mansur and H. S. Mansur, Characterization and in vitro release of cyclosporine-A from poly(D,L-lactide-co-glycolide implants obtained by solvent/extraction evaporation, *Quim. Nova*, 2012, **35**, 723–727.
54 T. Gulsun, S. E. Borna, I. Vural and S. Sahin, Preparation and characterization of furosemide nanosuspensions, *J. Drug Delivery Sci. Technol.*, 2018, **45**, 93–100.
55 Y. Iyama, M. Mineda, S. Sei, W. Hirasawa, Y. Matahira, Y. Seto, H. Sato and S. Onoue, Cyclosporine a-loaded UniORV®: Pharmacokinetic and safety characterization, *Int. J. Pharm.*, 2019, **570**, 118630.

56 M. Alwadei, M. Kazi and F. K. Alanazi, Novel oral dosage regimen based on self-nanoemulsifying drug delivery systems for codelivery of phytochemicals – Curcumin and thymoquinone, *Saudi Pharm. J.*, 2019, **27**, 866–876.

57 K.-O. Choi, N. P. Aditya and S. Ko, Effect of aqueous pH and electrolyte concentration on structure, stability and flow behavior of non-ionic surfactant based solid lipid nanoparticles, *Food Chem.*, 2014, **147**, 239–244.